J Mater Sci (2008) 43:6016–6019
DOI 10.1007/s10853-008-2910-9

LETTER

Effect of particle size distribution on microstructure and piezoelectric properties of MnO_2-added $0.95(K_{0.5}Na_{0.5})NbO_3$–$0.5BaTiO_3$ ceramics

Cheol-Woo Ahn · Sahn Nahm · Myong-Jae Yoo · Hyeung-Gyu Lee · Shashank Priya

Received: 25 January 2008 / Accepted: 28 July 2008 / Published online: 13 August 2008

At present, there are four prominent lead-free systems for actuator applications, which have been modified by various additives for enhancing the performance, namely, $(Na_{1/2}Bi_{1/2})TiO_3$–$(K_{1/2}Bi_{1/2})TiO_3$ (NBT–KBT), $(Na_{1/2}Bi_{1/2})TiO_3$–$BaTiO_3$ (BT), $(Na_xK_yLi_{1-x-y})NbO_3$ (KNLN), and $(Na_{1/2}K_{1/2})NbO_3$–$BaTiO_3$ (KNN–BT) [1–14]. Table 1 shows the representative properties of these four systems. Our research is focused on the KNN–BT system because of its potential to provide high piezoelectric and dielectric constants. In this letter, we address the synthesis issue for these compositions to obtain reliable and repeatable performance. This is a critical issue in order for research to converge and transition into products.

By conventional solid-state synthesis, 0.95KNN–0.5BT + x mol% MnO_2 ($0.0 \leq x \geq 2.0$) were prepared from oxides of >99% purity. The oxide powders of K_2CO_3, Na_2CO_3, Nb_2O_5, $BaCO_3$, and TiO_2 (all from High Purity Chemicals, Saitama, Japan) were mixed for 24 h in a nylon jar with zirconia balls. The mixed powders were dried and calcined at 950 °C for 3 h. Calcined powders were milled with MnO_2 (High Purity Chemicals, Saitama, Japan) for 24 h (MP1) and 48 h (MP2), and dried (see Table 2 for the abbreviations). The particle size distribution of raw and ball-milled 0.95KNN–0.5BT powders (P1 and P2) was measured with Mastersizer Micro and Microplus (Malvern Instruments Ltd., Malvern, UK) in the range of 0.05–1,000 μm. Dried powders were pressed into disks under a pressure of 100 kgf/cm^2, and the specimens were sintered in the range of 1,000–1,100 °C for 2 h. The crystal structure and microstructure of the specimens were examined by Rigaku D/max-RC X-ray diffractometer and Hitachi S-4300, Japan, scanning electron microscopy. The densities of the sintered specimens were measured by water-immersion technique. The samples were poled in silicone oil at 120 °C by applying a dc field of 4 kV/mm for 60 min. All electrical measurements were carried 24 h after poling. The electromechanical and piezoelectric properties were determined using a piezo d_{33} meter (Micro-Epsilon Channel Product DT-3300, Raleigh, NC) and an impedance analyzer (Agilent Technologies, Model HP 4194, Santa Clara, CA).

It is well known that the packing density of a green body directly influences sintering. The packing density is dependent on the ratio of small to large particles present in the mixture. Bimodal distribution is useful if there is a large difference in the size of the two groups, since the packing density can be increased by filling the interstitial holes between the larger particles with smaller size particles. It is also known that if the mixture has particles of three sizes with specific size ratios then packing is further improved. Furnas model shows that the maximum packing density in the green body occurs for the mixture containing 70% of the large particles [15]. However, results by German have shown that in certain cases, maximum density in the sintered body may occur for mixture containing 100% small particles [16, 17]. For a spherical geometry, it has been shown that the reaction rate is dependent on the particle size as [18]:

C.-W. Ahn · S. Priya (✉)
Department of Materials Science and Engineering, Virginia Polytechnic Institute and State University, Blacksburg, VA 24061, USA
e-mail: spriya@mse.vt.edu

S. Nahm · M.-J. Yoo
Department of Materials Science and Engineering, Korea University, 1-5 Ka, Anam-Dong, Sungbuk-Ku, Seoul 136-713, South Korea

M.-J. Yoo · H.-G. Lee
Korea Electronics Technology Institute, 68 Yatap-dong, Bundang-gu, Soeongnam-si, Gyeonggi-do 463-816, South Korea

Table 1 Room temperature dielectric and piezoelectric properties of prominent lead free systems

System	d_{33} (pC/N)	$\varepsilon_{33}/\varepsilon_o$	tan δ	k_p
NBT–KBT–BT [1]	183	770	0.034	0.367
NBT–KBT–LBT [2]	216	1,550	0.034	0.401
KNN–$LiSbO_3$ [3]	283	1,288	0.019	0.50
KNN–BT [6, 10]	225	1,058	0.033	0.36

LBT: $(Li_{0.5}Bi_{0.5})TiO_3$

Table 2 Abbreviations used in this paper

Abbreviation	Details
P1	0.95KNN–0.05BT (milling time: 24 h)
P2	0.95KNN–0.05BT (milling time: 48 h)
MP1	0.95KNN–0.05BT + 0.0–1.5 mol% MnO_2 (milling time: 24 h)
MP2	0.95KNN–0.05BT + 0.0–1.5 mol% MnO_2 (milling time: 48 h)

$$[1+(Z-1)\alpha]^{2/3}+(Z-1)(1-\alpha)^{2/3} = Z+(1-Z)\left(\frac{KD}{r^2}\right)t \quad (1)$$

where α is the fraction of volume that has already reacted to form the product, Z is the volume of particle formed per unit volume of the spherical particle which is consumed, D is the diffusion coefficient for rate limiting species, r is the particle size, t is the time, and K is the constant determined by chemical potential difference for the species diffusing across the reaction layer and geometry. Based on this expression, it can be seen that the rate of reaction is inversely proportional to the square of particle size ($1/r^2$). In a multi-component system, this becomes an important attribute as the reaction rate will be dependent on the largest particle sizes.

Figure 1a shows the particle size distribution of raw commercial powders (Na_2CO_3, K_2CO_3, Nb_2O_5, $BaCO_3$, and TiO_2) used in this work. There is a significant size difference between Na_2CO_3 and K_2CO_3 powders and the rest of the components. Particle sizes of Nb_2O_5, $BaCO_3$, and TiO_2 powders, were small <20 μm, compared with that of Na_2CO_3 and K_2CO_3 powders which were extremely large ~200 μm (about 10 times size difference). This result indicates that commercial alkali powders require significant reduction in size before being used to form the green body in order to avoid agglomeration. Thus, we next investigated the effect of the milling time on the particle size.

Figure 1b shows the variation of calcined particle size for two different milling times, 24 h and 48 h, referred as P1 and P2. Figure 2 shows the XRD plots of MnO_2 (x mol%)-added P1 and P2. Pure perovskite phase was observed in all the cases. From Fig. 1b, it can be seen that after 24 h of milling, the mixture (P1) consisted of bimodal distribution of particles. About ~44% of the particles had an average size of 0.3 μm and 46% of the particles had an average size of 30 μm. Since the initial particle size of Na_2CO_3 and K_2CO_3 powders was much larger than that of other powders, it could be responsible for the bimodal distribution. In case of P2 (milling time = 48 h), the volume fraction of small particles increased significantly to ~80%. Three particle sizes were observed in the mixture as shown in Fig. 1b, with high volume fraction of the particles having mean size of 0.3 μm.

The sintering temperatures of P1 and P2 modified with x mol% MnO_2 (MP1, MP2) were fixed at 1,100 and 1,050 °C based upon the density measurements. The ceramics sintered at these temperatures showed highest density. Figure 2 shows the X-ray diffraction patterns for sintered MP1 and MP2. All the peaks were indexed in terms of pure perovskite unit cell with no trace of secondary phase. Figure 3 shows the sintered density of the MP1 mixture (P1 + x mol% MnO_2) indicating values of approximately 80%. In the case of MP2 mixture, the sintered density increased significantly to 95.5%. There is a ~15% difference in the sintered density of MP1 and MP2

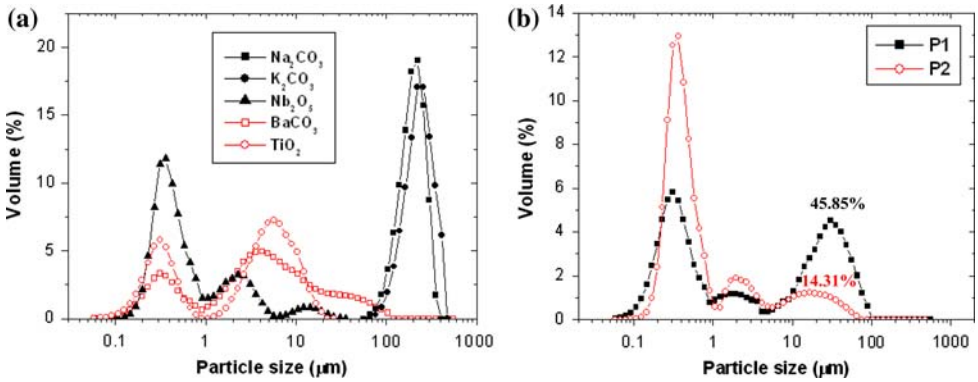

Fig. 1 Particle size distributions of (**a**) raw powders and (**b**) P1 and P2 powders

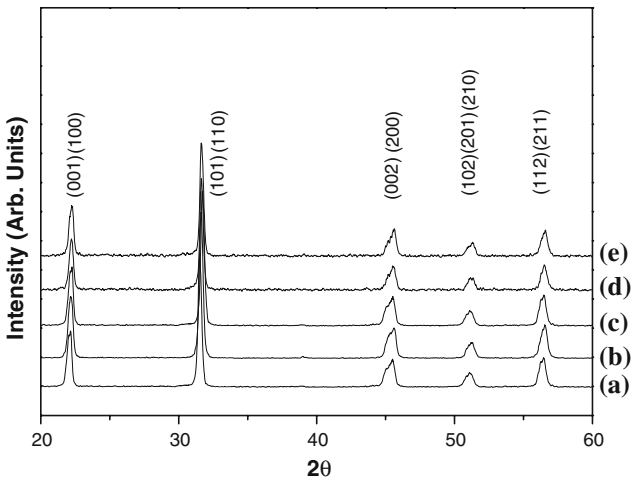

Fig. 2 X-ray diffraction patterns of x mol% MnO_2 added P1 specimens (MP1) sintered at 1,100 °C for 2 h and P2 specimens (MP2) sintered at 1,050 °C for 2 h: (a) MP1, $x = 0.0$, (b) MP1, $x = 0.9$, (c) MP2, $x = 0.0$, (d) MP2, $x = 0.5$, and (e) MP2, $x = 2.0$

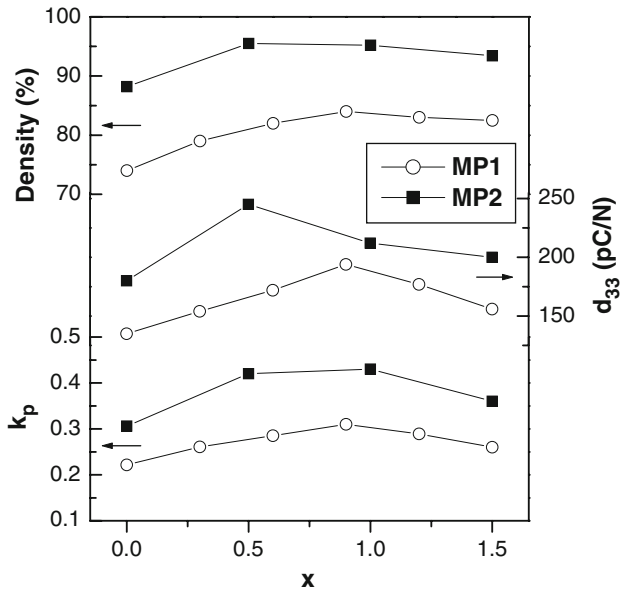

Fig. 3 Relative densities and piezoelectric properties of MP1 specimens sintered at 1,100 °C for 2 h and MP2 specimens sintered at 1,050 °C for 2 h

mixtures illustrating the significance of initial particle size distribution.

A recent result of Moskovits et al. also illustrates similar behavior for bimodal Y_2O_3-stabilized zirconia powder mixtures sintered at low temperatures [19]. These results indicate that for alkali niobate-based lead-free ceramics a higher density can be obtained by using higher content of smaller size particles (<0.3 μm) in the green body. This result can also be interpreted from German's model. In those cases where shrinkage of smaller particles is higher as compared to that of larger particles and particle size ratio is large (>100), it is better to have 100% small particles. An estimate on the shrinkage can be made obtained for the two cases studied here.

According to German's model, the change in specific volume (ΔV_m) during sintering is a function of mixture composition and is given as [17]:

$$\Delta V_m = \Delta V_s - (X/X_t)(\Delta V_S - \Delta V_L) \quad \text{for } X < X_t \tag{2}$$

where ΔV_s represents the change in specific volume of small particles and ΔV_L is the change in specific volume of the large particles, X is the content of large particles in the mixture, and X_t represents the composition where large particles form a continuous network with all the interstitial pores between the large particles saturated with small particles. The densification can be computed from the knowledge of specific volume of the green body (V_g) as follows:

$$\Phi = \frac{\Delta V_m}{\left[(V_g - 1)(V_g - \Delta V_m)\right]} \tag{3}$$

For the two cases studied here, $\Phi_1 = 0.80$, and $\Phi_2 = 0.95$, the specific change in volume of the mixture can be computed to be $\Delta V_m^1 = 0.4631$, and $\Delta V_m^2 = 0.6463$ by using $V_g^1 = 1/0.65$ (P1) and $V_g^2 = 1/0.60$ (P2).

Figure 4 shows the SEM images of sintered MP1 and MP2 specimens. The sintered MP1 specimens showed small grain sizes with an average size of 0.3 μm. However for sintered MP2 samples, grain growth occurred and large grains of average size 1.0–3.0 μm were found as shown in Fig. 4c and d. These results indicate that small particles provide better densification through uniform grain growth.

Figure 3 also summarizes the variation of piezoelectric properties for sintered MP1 and MP2 specimens along with density. The variation of piezoelectric properties was similar to that of density indicating that density plays an important role toward piezoelectric properties of alkali niobate-based ceramics. Excellent piezoelectric properties of $d_{33} = 245$ pC/N and $k_p = 0.42$ were observed for 0.95KNN–0.05BT + 0.5 mol% MnO_2 ceramics sintered at 1,050 °C for 2 h. These results are quite promising for the lead-free piezoelectrics.

In summary, the effect of particle size distribution on the microstructure and piezoelectric properties of 0.95KNN–0.05BT + x mol% MnO_2 ceramics was investigated in this letter. In order to improve the grain growth and density, particle size of 0.95KNN–0.05BT powder was controlled. It was found that a high volume fraction of small size particles enhances the sintered density. Based on the results, it is proposed that higher piezoelectric properties in this system can be obtained by using 100% particles of size less than 0.3 μm in the green body.

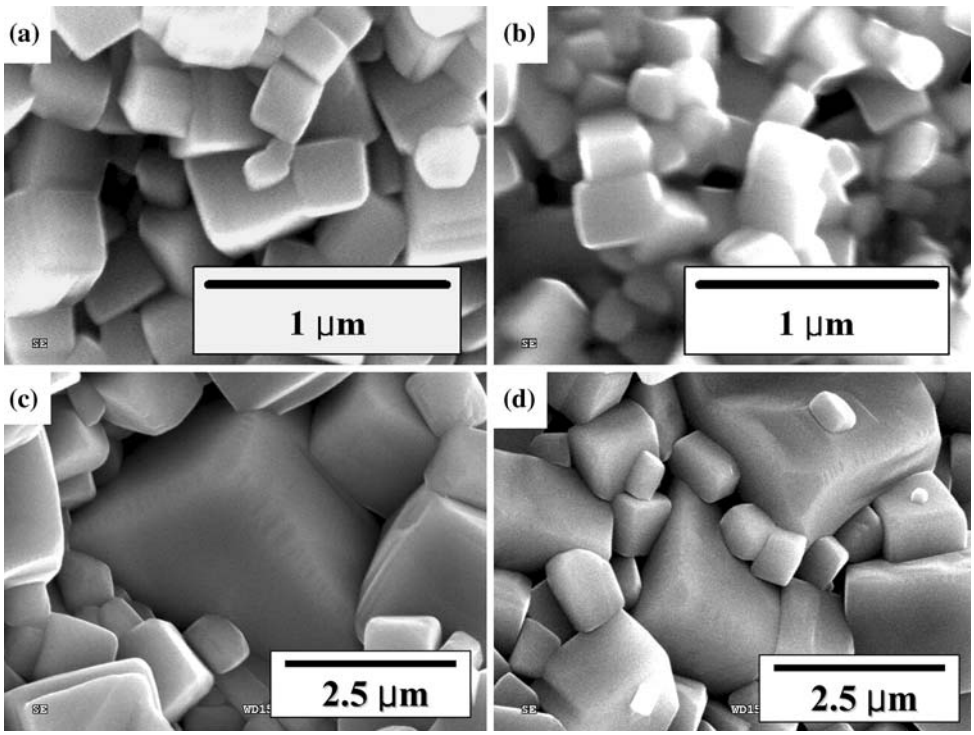

Fig. 4 SEM images of MP1 specimens sintered at 1,100 °C for 2 h and MP2 specimens sintered at 1,050 °C for 2 h: (**a**) MP1, $x = 0.0$ (**b**) MP1, $x = 0.9$, (**c**) MP2, $x = 0.0$, and (**d**) MP2, $x = 0.5$

Acknowledgements The authors (C.-W. A. and S. P.) gratefully acknowledge the financial support from Office of Basic Energy Science, Department of Energy.

References

1. Takenaka T, Nagata H (2005) J Eur Ceram Soc 25:2693. doi:10.1016/j.jeurceramsoc.2005.03.125
2. Yuan Y, Zhang S, Zhou X, Liu J (2006) Jpn J Appl Phys 45:831. doi:10.1143/JJAP.45.831
3. Zang GZ, Wang JF, Chen HC, Su WB, Wang CM, Qi P et al (2006) Appl Phys Lett 88:212908. doi:10.1063/1.2206554
4. Saito Y, Takao H, Tani T, Nonoyama T, Takatori K, Homma T et al (2004) Nature 432:84. doi:10.1038/nature03028
5. Park SH, Ahn CW, Nahm S, Song JS (2004) Jpn J Appl Phys 43:L1072. doi:10.1143/JJAP.43.L1072
6. Park HY, Ahn CW, Song HC, Lee JH, Nahm S, Uchino K et al (2006) Appl Phys Lett 89:062906-1. doi:10.1063/1.2335816
7. Song HC, Cho KH, Park HY, Ahn CW, Nahm S, Uchino K, Lee HG (2007) J Am Ceram Soc 90(6):1812. doi:10.1111/j.1551-2916.2007.01698.x
8. Park HY, Ahn CW, Cho KH, Nahm S, Lee HG, Kang HW et al (2007) J Am Ceram Soc 90(12):4066
9. Cho KH, Park HY, Ahn CW, Nahm S, Lee HG, Lee HJ (2007) J Am Ceram Soc 90(6):1946. doi:10.1111/j.1551-2916.2007.01715.x
10. Ahn CW, Park HY, Nahm S, Uchino K, Lee HG, Lee HJ (2007) Sens Actuators A 136:255
11. Ahn CW, Song HC, Nahm S, Park SH, Uchino K, Priya S et al (2005) Jpn J Appl Phys 44(44):L1361. doi:10.1143/JJAP.44.L1361
12. Guo Y, Kakimoto K, Ohsato H (2004) Jpn J Appl Phys 43:6662. doi:10.1143/JJAP.43.6662
13. Guo Y, Kakimoto K, Ohsato H (2004) Solid State Commun 129:279. doi:10.1016/j.ssc.2003.10.026
14. Guo Y, Kakimoto K, Ohsato H (2004) Appl Phys Lett 85(18):4121. doi:10.1063/1.1813636
15. Furnas CC (1931) Ind Eng Chem 23:1052. doi:10.1021/ie50261a017
16. German RM (1992) Metall Trans 23A:1455
17. German RM (1992) Acta Metall Mater 40(9):2085. doi:10.1016/0956-7151(92)90125-X
18. Carter E (1961) J Chem Phys 35:1137. doi:10.1063/1.1701201
19. Moskovits M, Ravi BG, Chaim R (1999) NanoStruct Mater 11(2):179